*Pure Appl. Chem.*, Vol. 77, No. 8, pp. 1331–1343, 2005.
DOI: 10.1351/pac200577081331


# Entropy diagnosis for phase transitions occurring in functional materials*

Michio Sorai‡

*Research Center for Molecular Thermodynamics, Graduate School of Science, Osaka University, Toyonaka, Osaka 560-0043, Japan*

*Abstract*: Functionalities of materials manifest themselves as the result of a concerted effect among molecular structure, intermolecular interactions, and molecular motions. Since the entropy of substance directly reflects the degree of molecular motions, the entropy plays a crucial role when one discusses the stability of a given phase at finite temperatures. When a delicate balance of these three factors is broken, the condensed state faces a catastrophe and is transformed into another phase. Therefore, phase transition is a good probe for elucidation of the interplay between these three factors. As there is no selection rule in thermodynamics, the entropy gain at the phase transition is a good tool to diagnose the mechanism of phase transition. In this presentation, calorimetric investigations aimed at the elucidation of the mechanisms governing phase transitions occurring in molecule-based functional materials are reviewed.

*Keywords*: Entropy; phase transitions; functionalities of materials; entropy diagnosis; concerted effect; heat capacity calorimetry.

## INTRODUCTION

Condensed states of matter are basically controlled by the interplay among molecular structure, intermolecular interactions, and molecular motions. Functionalities of materials manifest themselves as the result of a concerted effect among these three factors. The former two factors are always taken into account in theories and models for interpretation of experimental facts. However, the molecular motions are often forgotten or neglected in those treatments, because they are difficult to treat. Molecular motions are directly reflected in the entropy of substances, and, thus, the Gibbs energy is modulated. Therefore, as far as one discusses the stability of a given phase at finite temperatures, the molecular motions play a crucial role. When the delicate balance of these three factors is broken, the condensed state faces a catastrophe and is transformed into another phase, the so-called phase transition. Therefore, phase transition is a good probe for elucidation of the interplay among these three factors. On the other hand, the entropy gain at the phase transition plays a diagnostic role for interpretation of the mechanisms governing the phase transitions.

In this presentation, calorimetric investigations aimed at the elucidation of the mechanisms of phase transitions occurring in molecule-based functional materials are reviewed [1–6].

---

*Paper based on a presentation at the 18th IUPAC International Conference on Chemical Thermodynamics (ICCT-2004), 17–21 August 2004, Beijing, China. Other presentations are published in this issue, pp. 1297–1444. Contribution No. 86 from the Research Center for Molecular Thermodynamics.
‡E-mail: sorai@chem.sci.osaka-u.ac.jp

## ENTROPY DIAGNOSIS FOR PHASE TRANSITIONS

### Molecule-based magnet: Pure organic radical

The first example is a molecule-based magnet consisting of pure organic radical, 4-methacryloyloxy-2,2,6,6-tetramethylpiperidin-1-oxyl (MOTMP: Fig. 1) [7–9]. The unpaired electron is mainly localized on the terminal oxygen atom. The magnetic susceptibility of this crystal detected the existence of ferromagnetic interaction between the neighboring radicals. Figure 2 shows its heat capacity as a function of temperature in logarithmic scales. At high temperatures, the heat capacity consists of the contribution from nonmagnetic lattice vibrations shown by the curve (1). This contribution is suppressed with decreasing temperature. Below 3 K, however, the heat capacity is increased in spite of cooling as shown by curve (2), and eventually a phase transition occurs at 0.14 K.

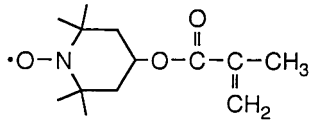


**Fig. 1** Molecular structure of MOTMP.

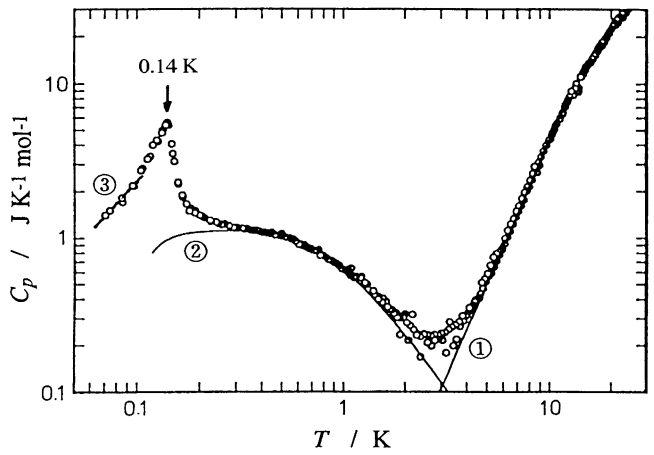


**Fig. 2** Molar heat capacity of molecule-based magnet MOTMP. Curve (1): Lattice heat capacity. Curve (2): 1D Heisenberg ferromagnetic chain ($J_{intra}/k$ = 0.45 K). Curve (3): Spin-wave contribution ($T^{1.53} \approx T^{3/2}$) [7,8].

Since the molecule-based magnets consist of molecular parts as the building blocks, their structures are anisotropic and, thus, physical properties such as magnetic interactions inevitably become anisotropic. This leads to low-dimensional magnets in which one- or two-dimensional interaction is dominant. Short- and long-range orders formed by spins crucially depend on the magnetic lattice structure. These features are very sensitively reflected in heat capacity. This broad anomaly unexpectedly observed is well accounted for in terms of the short-range-order effect of the spin orientation in ferromagnetic Heisenberg chains with the intrachain interaction parameter of $J_{intra}/k$ = 0.45 K, where $k$ is the Boltzmann constant. As far as its crystal structure is concerned [8], there seems to be no indication of favorable paths of one-dimensional (1D) magnetic interactions. This fact clearly indicates the high sensitivity of the heat capacity to the dimensionality. This finding of dominant one-dimensional behavior was afterwards confirmed by magnetic susceptibility measurements done below 1 K [10].

The entropy due to the magnetic phase transition and the broad anomaly was 5.81 J $K^{-1}$ $mol^{-1}$. Since the observed entropy gain agrees well with $R$ ln 2 = 5.76 J $K^{-1}$ $mol^{-1}$, one can know the origin of the phase transition is surely the spin alignment.

## Thermochromic compound: $[Cu(daco)_2](NO_3)_2$

Some transition-metal compounds change color in the solid state depending on temperature. This phenomenon is known as thermochromism. An example is the square-planar copper(II) complex $[Cu(daco)_2](NO_3)_2$, where daco = 1,5-diazacyclooctane. The ligand "daco" (see Fig. 3) is an eight-membered ring molecule. The color of this crystal is brilliant orange at room temperature, but it changes discontinuously to violet above 360 K and reverts to orange on cooling.

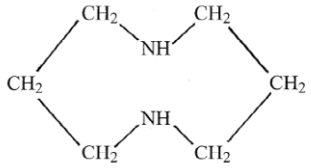


**Fig. 3** Molecular structure of ligand "daco".

Figure 4 shows the molar heat capacity of this compound [11]. A large heat capacity anomaly associated with the thermochromic phenomenon was found at 360 K. The entropy gain at the phase transition was as large as $\Delta S$ = 23.37 J $K^{-1}$ $mol^{-1}$. We anticipated that dynamic butterfly-motions of the daco-ligand might be responsible for the large entropy gain. Figure 5 shows four available conformations of a single daco-ligand with almost equal energy. Since this complex contains two daco-ligands per formula unit, the total number of available conformations becomes $4 \times 4 = 16$. If daco-ligands are conformationally ordered at low-temperature while dynamically disordered at high-temperature, the expected entropy gain due to the conformational disorder is $R \ln 16 = 23.05$ J $K^{-1}$ $mol^{-1}$. This value agrees surprisingly well with the observed entropy gain. This mechanism of phase transition was confirmed afterwards by use of proton NMR experiment.

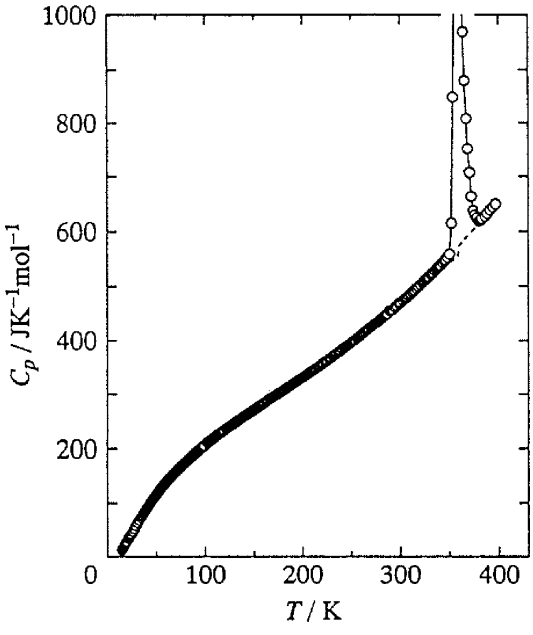


**Fig. 4** Molar heat capacity of the thermochromic compound $[Cu(daco)_2](NO_3)_2$ [11].

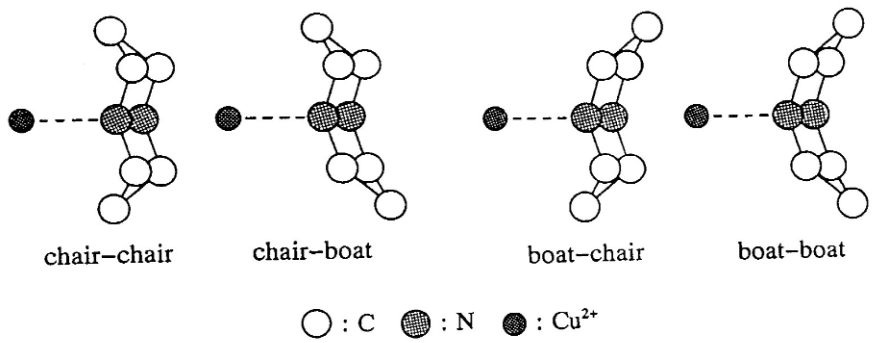


**Fig. 5** Four available conformations of a single daco ligand with almost equal energy [11].

## Halogen-bridged 1D mixed-valence compound: $[Pt^{II}Pt^{III}(S_2CCH_3)_4I]$

Halogen-bridged mixed-valence dinuclear metal complexes, the so-called MMX chain compounds, have drawn attention as a useful candidate of functional materials manifesting various electronic states through possible charge-transfer mechanism. The platinum compound $[Pt^{II}Pt^{III}(S_2CCH_3)_4I]$ is a typical example of this category. Two platinum atoms are bridged by four bidentate dithioacetato ligands, and such binuclear complex units linearly bridged one another by iodide ions [12]. X-ray diffraction study [13] revealed that the plane formed by SCS atoms of a ligand is regularly tilted at room temperature, while above about 370 K, the ligand plane can randomly convert between two tilted directions available for right and left sides with equal probability.

Figure 6 shows the molar heat capacity of this material [14]. The structural phase transition was actually observed at 373.4 K. The entropy gain at this phase transition was only 5.64 J $K^{-1}$ $mol^{-1}$. If the four dithioacetato ligands reorient independently between two positions, the total entropy gain expected for the order–disorder phase transition would be $4 \times R \ln 2 = 23.05$ J $K^{-1}$ $mol^{-1}$. However, this is quite far from the observed value. The observed entropy is just 1/4 of the independent motion model. This fact clearly indicates that order–disorder motions of the four dithioacetato ligands might be synchronized. In that case, the theoretical entropy is only $R \ln 2 = 5.75$ J $K^{-1}$ $mol^{-1}$. This value agrees well with the observed value. Therefore, one can safely conclude that the ligand motions in this complex are not independent but synchronized.

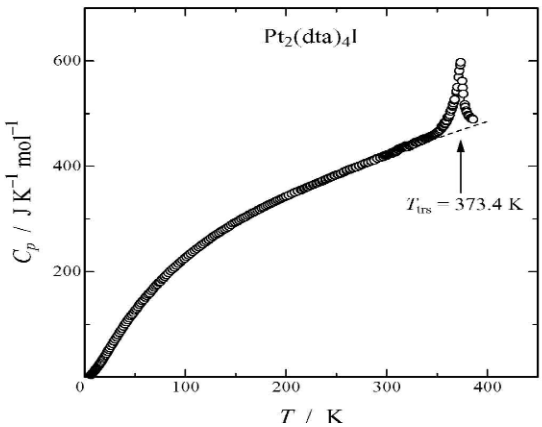


**Fig. 6** Molar heat capacity of the MMX-type mixed-valence complex $[Pt^{II}Pt^{III}(S_2CCH_3)_4I]$ [14].

### Charge-transfer quasi-1D-ferrimagnet: [MnT(R)PP][TCNE]

Another example of a molecule-based magnet are the charge-transfer complexes between manganese(III)-tetraphenylporphyrin and TCNE, [MnT(R)PP][TCNE]·(solv), where solv implies the solvent molecule. This system forms a quasi-1D-ferrimagnetic chain structure with the spin quantum numbers of 2 and 1/2, respectively. The compounds introduced here are those with (R = *n*-$C_{14}H_{29}$ and solv = MeOH) and (R = F and solv = 0.5MeOH). They exhibit the spontaneous magnetization below critical temperature $T_c$ = 20.5 K [15] and 27 K [16], respectively, and the AC magnetic susceptibility exhibits a very drastic change at the critical temperatures. One may naturally expect some heat capacity anomalies around the critical temperatures.

Recently, we measured heat capacities of these complexes. Figure 7 illustrates their molar heat capacities [17]. Quite mysteriously, we could not detect any heat capacity anomalies due to the magnetic ordering around 20 and 27 K. To solve this mystery, one should pay attention to the characteristic magnetic structure of these complexes. As schematically shown in Fig. 8, they consist of a quasi-1D-ferrimagnetic chain with a very strong antiferromagnetic interaction between the spin quantum number 2 of the manganese ion and the spin 1/2 of TCNE radical. Since there is no theoretical treatment of heat capacity of this type of ferrimagnetic system, we shall approximate the actual system by a simple antiferromagnetic chain with identical spin quantum number of 3/2. Figure 9 demonstrates the heat capacity of an antiferromagnetic chain with the intrachain interaction $J_{intra}/k = -150$ K. This hypothetical magnetic chain gives rise to a very broad heat capacity anomaly over a wide temperature region. The large entropy gained above ~20 K cannot contribute to the magnetic phase transition, because this entropy corresponds to the strong short-range order still remaining above $T_c$. The entropy available for the phase transition is a very small part below ~20 K. This is the reason for substantially no effect in the heat capacity.

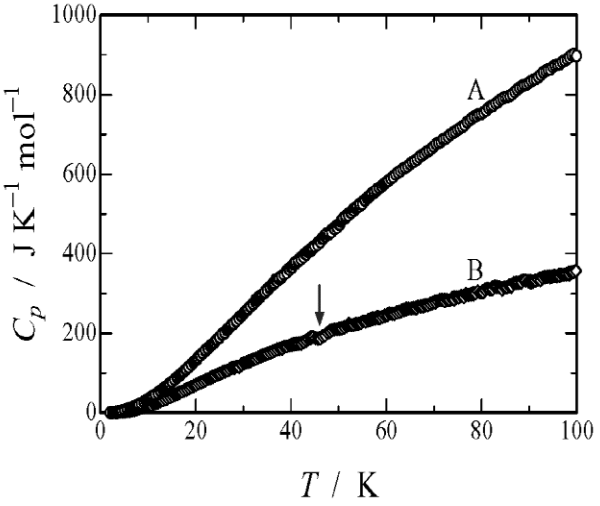


**Fig. 7** Molar heat capacity of [MnT(R)PP][TCNE]·(solv). Curve A: R = *n*-$C_{14}H_{29}$ and solv = MeOH. Curve B: R = F and solv = 0.5 MeOH [17].

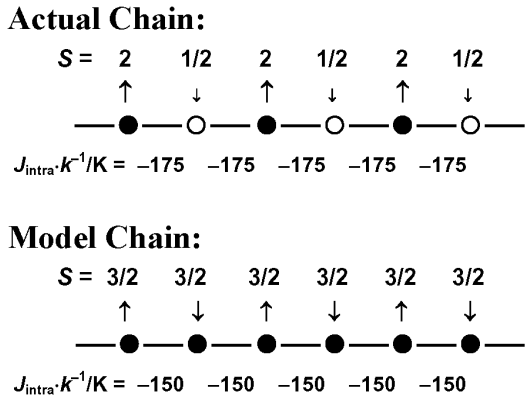


**Fig. 8** Schematic drawing of the characteristic magnetic structure of the complex [MnT(R)PP][TCNE]·(solv).

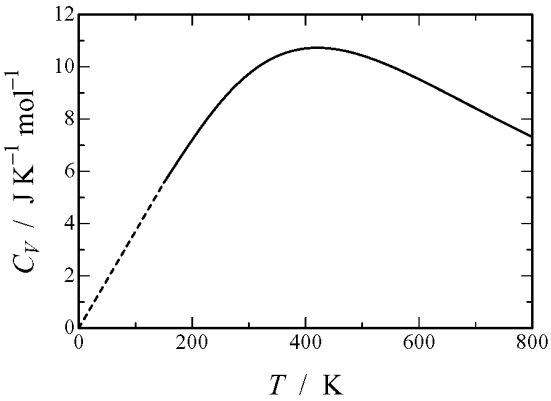


**Fig. 9** The heat capacity of an antiferromagnetic chain with the intrachain interaction $J_{intra}/k = -150$ K.

However, there still remains a big mystery. Why is an enhanced effect possible for magnetic susceptibility, while there is substantially no effect in the heat capacity? To solve this mystery, we anticipated formation of magnetic domains in the actual crystal. To simplify the situation, we shall assume the following model: (1) Antiferromagnetically coupled pair of spins ($S$ = 2 and 1/2) form a resultant spin ($S$ = 3/2). (2) The resultant spins have a tendency to form ferromagnetic short-range order. A region of the short-range order is assumed to form a magnetic domain of uniform size. (3) The number of spins in a domain is $n$. (4) Under zero magnetic field, the net magnetic moments of domains fluctuate paramagnetically. The number of domains with up-spin and down-spin are designated as $N_D(\uparrow)$ and $N_D(\downarrow)$, respectively. These numbers are related to the Avogadro constant $N_A$ through the following equation,

$$[N_D(\uparrow) + N_D(\downarrow)]\cdot n = N_A \tag{1}$$

As the magnetization $M$ is proportional to the effective number of spins orienting to the magnetic field, it is expressed by the equation,

$$M \propto [N_D(\uparrow) - N_D(\downarrow)]\cdot n = N_A\cdot[N_D(\uparrow) - N_D(\downarrow)] \,/\, [N_D(\uparrow) + N_D(\downarrow)] \tag{2}$$

Since the parameter $n$ does not appear in the final form of the magnetization equation, the formation of domain does not influence the magnetization at all.

On the other hand, when the magnetic domains are formed, the magnetic susceptibility $\chi$ is given by the following equation,

$$\chi = (N_A/n)\cdot[(n\cdot\mu_{eff})^2/3kT] = n\cdot[N_A\cdot\mu_{eff}{}^2/3kT] \quad (3)$$

where $\mu_{eff}$ means the effective magnetic moment of a single spin. From this equation, one can know that the magnetic susceptibility is enhanced in proportion to $n$. Consequently, the enhanced effect observed in the magnetic susceptibility is compatible with the assumption of the formation of magnetic domains in the crystal.

### Neutral–ionic transition in TTF–CA

The next subject is a phase transition occurring in a charge-transfer mixed-stack complex of tetrathiafulvalene (TTF) and *p*-chrolanil (CA). TTF serves as an electron donor, while CA is an electron acceptor. However, the electron transfer is incomplete in this complex. About 0.3 electron is transferred from the donor to the acceptor at room temperature. Since the degree of charge transfer is less than 0.5, this state is designated as quasi-neutral. When the temperature of the crystal is decreased, additional charge transfer occurs around 80 K, and the degree of the electron transfer is increased to 0.7. This state is regarded as quasi-ionic. Namely, this complex undergoes the so-called neutral-to-ionic (NI) transition.

Figure 10 shows the molar heat capacities of TTF–CA prepared by cosublimation method [18]. A very sharp heat capacity peak due to the NI transition was observed at 82.5 K. The entropy gain was $\Delta S$ = 6.12 J K$^{-1}$ mol$^{-1}$. Judging from the transition entropy, one can surely assume that the NI transition is not of displacement type but of order–disorder type. However, X-ray and neutron diffraction studies have not detected any structural disorder in TTF–CA crystals [19,20]. Therefore, a plausible explanation for the origin of this large entropy change is softening of the acoustic lattice vibrations on going from the low-temperature ionic phase to the high-temperature neutral phase, namely, the change in the lattice vibrations along the 1D stacking direction are probably responsible for the large entropy gain.

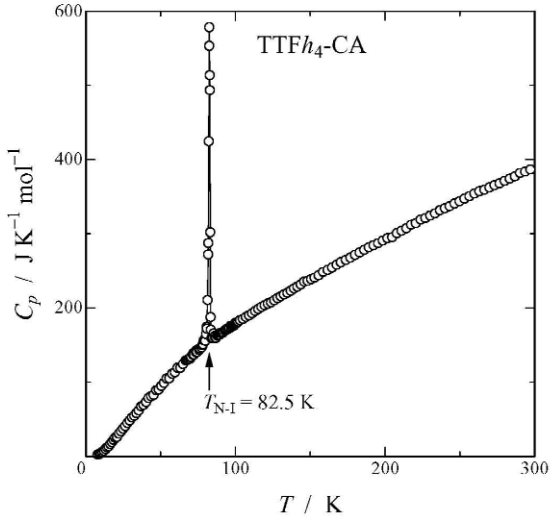


**Fig. 10** Molar heat capacity of TTF–CA prepared by cosublimation method [18].

### Spin-crossover phenomena

Some transition-metal ions can exist either in high- or low-spin ground state depending on the ligand-field strength. For example, when Fe(II) ion is located in an octahedral $O_h$ ligand field, its six d-elec-

trons are accommodated in the $t_{2g}$ and $e_g$ orbitals in accordance with the Pauli principle and the Hund rule. Since the number of unpaired electrons is four, the net spin quantum number becomes 2 (the high-spin state). On the other hand, when the ligand field is strong, all the electrons are accommodated in the ground $t_{2g}$ orbitals against the Hund rule. In this case, the spin quantum number becomes 0 (the low-spin state). Spin-state transition can occur between these two spin states when the ligand-field strength is close to the electron-pairing energy. When the spin state is altered by temperature or pressure, the phenomenon is called "spin crossover" [21].

Since the spin-crossover phenomenon is principally based on a change in the electronic state, many researchers believed that the dominant driving force leading to temperature-induced spin-crossover transition would be a change in the spin multiplicity. However, based on heat capacity measurements on spin-crossover complex $[Fe^{II}(NCS)_2(phen)_2]$, where phen = 1,10-phenanthroline, we claimed that this interpretation is not reasonable [22,23]. The molar heat capacity is reproduced in Fig. 11. This complex exhibited a big phase transition at 176.29 K owing to the spin-crossover phenomena. The observed entropy gain at the phase transition was as large as 48.78 J $K^{-1}$ $mol^{-1}$, which is much larger than the entropy gain owing to the change in the spin multiplicity from singlet (LS state) to quintet (HS state) ($R$ ln 5 = 13.38 J $K^{-1}$ $mol^{-1}$). The remaining entropy of about 36 J $K^{-1}$ $mol^{-1}$ is accounted for in terms of the phonon entropy mainly due to the metal–ligand skeletal vibrational modes, because the bond lengths are dramatically elongated on going from low- to high-spin state. This dramatic change in the vibrational frequencies can easily be seen in the variable-temperature IR and Raman spectra. One can, therefore, conclude that the spin-crossover phenomena takes place as the result of strong coupling between the electronic state and the phonon systems.

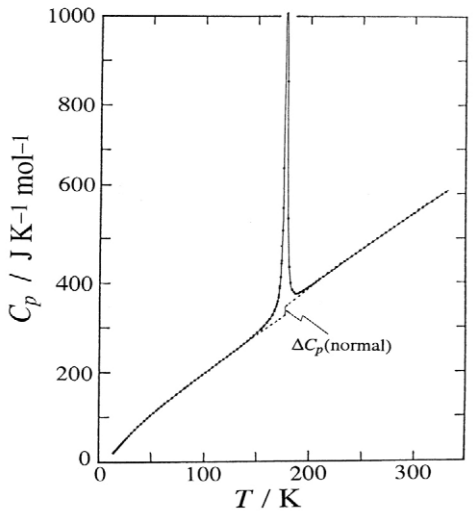


**Fig. 11** Molar heat capacity of the abrupt-type spin-crossover complex $[Fe^{II}(NCS)_2(phen)_2]$ [22,23].

As is well known, temperature-induced spin-crossover phenomena are classified into two types: one is the so-called "abrupt type", and the other is the "gradual type". The spin-crossover complex $[Fe(2\text{-pic})_3]Cl_2 \cdot MeOH$, where 2-pic = 2-picolylamine or 2-aminomethyl-pyridine, corresponds to the gradual type. As shown in Fig. 12, this complex gives rise to a broad heat capacity anomaly centered around 150 K [24]. The entropy gain due to the anomaly was as large as 59.5 J $K^{-1}$ $mol^{-1}$, indifferent of the sharpness of the spin crossover. To elucidate the reason for the gradual spin-state conversion, we proposed a domain model (see Fig. 13), which assumes that a crystal lattice consists of noninteracting domains with uniform size containing the identical number of complexes and that the spin-state conversion in each domain takes place simultaneously in the unit of domain. As the number of spins in a

domain $n$ is decreased, the heat capacity peak due to the spin crossover becomes broader and the cooperativity of the transition becomes weaker. When $n$ takes the extreme value unity, the system just corresponds to a chemical equilibrium described by the van't Hoff scheme. The existence of such domains was evidenced for the ethanol-solvate complex $[Fe(2\text{-pic})_3]Cl_2 \cdot EtOH$ based on EPR measurements in 1990 by Doan and McGarvey [25].

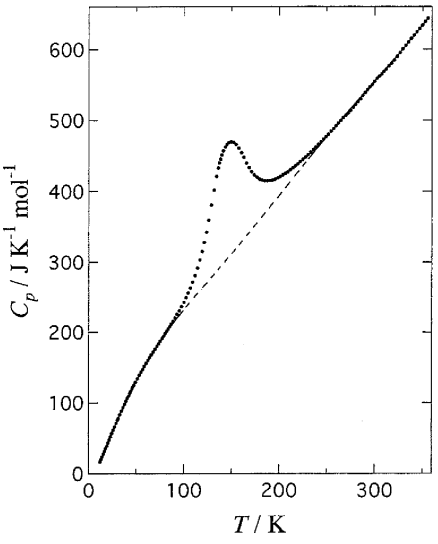


**Fig. 12** Molar heat capacity of the gradual-type spin-crossover complex $[Fe(2\text{-pic})_3]Cl_2 \cdot MeOH$ [24].

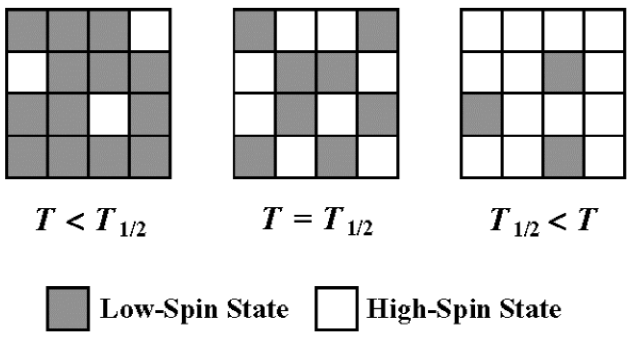


**Fig. 13** Noninteracting domain model with uniform size [23]. $T_{1/2}$ indicates the temperature at which the low-spin fraction becomes equal to the high-spin fraction.

The excess heat capacity of this complex beyond the normal heat capacity is given in Fig. 14. The excess heat capacity is well reproduced by the domain model (solid curve) when the number of complex in a domain is only $n = 1.5$. This small number of complex per domain makes a sharp contrast to 95 for $[Fe(NCS)_2(phen)_2]$ [23] and 2000 for $[CrI_2(depe)_2]$, where depe = *trans*-bis[1,2-bis-(diethylphosphino)ethane] [26], which belongs to the abrupt-type complex. The present result implies that the cooperativity in the complex $[Fe(2\text{-pic})_3]Cl_2 \cdot MeOH$ is extremely weak or absent.

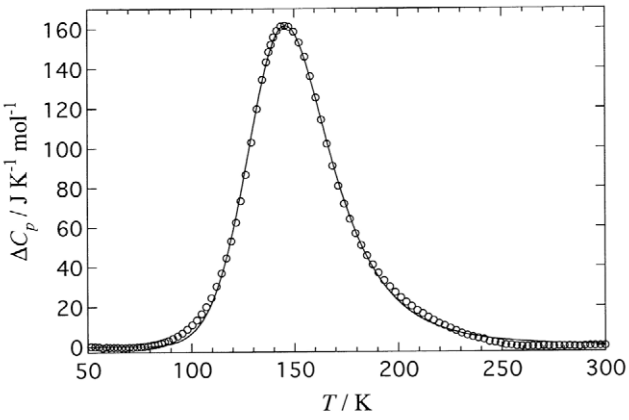


**Fig. 14** The excess heat capacity of $[Fe(2\text{-pic})_3]Cl_2 \cdot MeOH$ beyond the normal heat capacity. The solid curve corresponds to the domain model with $n = 1.5$ [24].

## Charge-transfer phase transition with spin-state conversion

The last topic is the mixed-valence assembled-metal complex $\{(n\text{-}C_3H_7)_4N[Fe^{II}Fe^{III}(dto)_3]\}_\infty$, where dto = dithiooxalato, reported by Kojima et al. [27,28] (Fig. 15). This complex consists of Fe(II) and Fe(III) ions. They are bridged by dithiooxalato ligands. Each iron ion is octahedrally coordinated either by six oxygen atoms or by six sulfur atoms. Since the ligand field at the sulfur site is much stronger than that at the oxygen site, the iron ion surrounded by sulfur atoms is characterized by low-spin state, while that surrounded by oxygen atoms shows high-spin state. X-ray diffraction study reveals that this assembled-metal complex forms a 2D layer structure. For charge balance, tetrapropyl-ammonium cations are inserted between the layers.

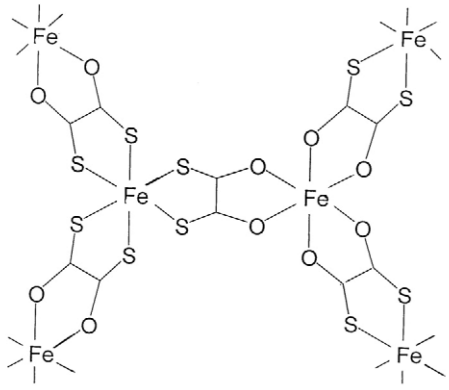


**Fig. 15** The mixed-valence assembled-metal complex $\{(n\text{-}C_3H_7)_4N[Fe^{II}Fe^{III}(dto)_3]\}_\infty$.

As shown in Fig. 16, at room temperature, iron ion at the sulfur site is low-spin Fe(III) with spin quantum number $S = 1/2$, while that at the oxygen site is high-spin Fe(II) with $S = 2$. When the temperature is decreased, electron transfer occurs from the oxygen site to the sulfur site around 110 K and their oxidation states are converted. As a result, the iron ion at the oxygen site becomes high-spin Fe(III) with $S = 5/2$ and that at the sulfur site is low-spin Fe(II) with $S = 0$. On the other hand, when the temperature of crystal is increased, the electron is inversely transferred around 120 K from the sulfur site

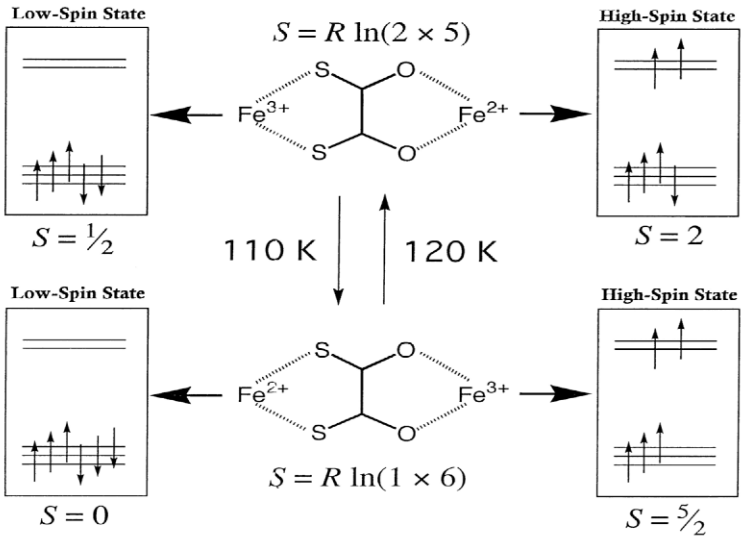


**Fig. 16** The electron transfer and spin-state conversion in $\{(n\text{-}C_3H_7)_4N[Fe^{II}Fe^{III}(dto)_3]\}_\infty$ [27–29].

to the oxygen site. It is clear that the spin multiplicity at the high-temperature phase is $2 \times 5 = 10$, while that at the low-temperature phase is $1 \times 6 = 6$.

Figure 17 is the observed molar heat capacity of this complex. Three anomalies were observed: A sharp peak at 122.4 K, a broad heat capacity anomaly centered at 253.5 K, and a very small anomaly around 7 K due to the magnetic ordering. The heat capacity anomaly at 253.5 K can be attributed to the order–disorder type of phase transition due to conformational changes in tetrapropyl-ammonium cation, because similar heat capacity anomalies have also been observed in some analogous molecule-based magnets having tetrabutyl-ammonium cations.

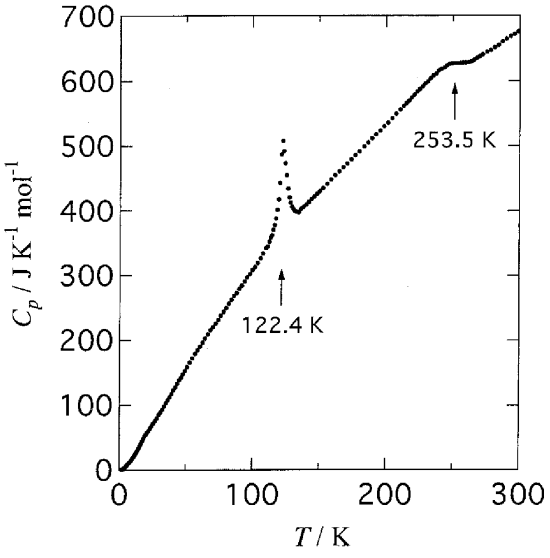


**Fig. 17** Molar heat capacity of $\{(n\text{-}C_3H_7)_4N[Fe^{II}Fe^{III}(dto)_3]\}_\infty$ [29].

The anomaly at 122.4 K obviously arises from the electron-transfer phenomenon, because the transition temperature agrees well with the temperature at which the anomaly is observed in the magnetic susceptibility and the Mössbauer spectroscopy. It should be remarked here that the entropy gain at the phase transition is very small, only 9.2 J $K^{-1}$ $mol^{-1}$, in spite of a big event including the electron transfer. The entropy gain due to the change in the spin multiplicity is $R$ ln (10/6) = 4.3 J $K^{-1}$ $mol^{-1}$.

The remaining small entropy of about 5 J $K^{-1}$ $mol^{-1}$ may be accounted for as follows. In the case of usual spin crossover, the bond lengths between the central metal atom and the ligands are basically determined by the spin state. Contrary to this, the bond lengths in the present complex are determined by the oxidation state of the metal ion. The bond length between the metal ion and the ligand is shorter when the oxidation state of the metal ion is high. As shown in Fig. 16, the oxidation state of iron ion at the oxygen site is three in the low-temperature (LT) phase while two in the high-temperature (HT) phase. Therefore, the bond length between iron and oxygen atoms is shorter in the LT phase than in the HT phase. Contribution of the skeletal vibrations to the entropy is greater in the HT phase than in the LT phase. This is quite a normal tendency in the sense that the entropy of the HT phase is greater than that of the LT phase. On the other hand, the oxidation state at the sulfur site is two in the LT phase, whereas three in the HT phase. In this case, the vibrational entropy is smaller in the HT phase than in the LT phase. Since these vibrational entropies at the oxygen and the sulfur sites contribute oppositely to the entropy change when the electron transfer occurs, both contributions would cancel out each other. The imbalance part of the cancellation seems to be the origin of the small excess entropy beyond the contribution from the change in the spin multiplicity.

## CONCLUDING REMARKS

Thermodynamics is not restricted by any selection rules, and, thus, thermodynamic quantities contain contributions from all kinds of molecular degrees of freedom in accordance with the Boltzmann distribution. Consequently, thermodynamics has a wide applicability of its concepts. This makes a sharp contrast to various spectroscopies in which particular nuclide and/or particular modes are selectively sensed.

Although the entropy diagnosis introduced here seems to be a rather classical research subject, it still displays great powers in understanding materials science. I would like to close my presentation by concluding as follows: (1) "Phase transition" is a good probe for elucidation of the interplay between molecular structure, intermolecular interactions, and molecular motions. (2) The "entropy" gained at the phase transition plays a diagnostic role to interpret the mechanisms governing the phase transitions. (3) The importance of "molecular thermodynamics" encompassing the macroscopic and the microscopic aspects should be emphasized for the studies of functional materials.

## ACKNOWLEDGMENTS

These studies have been performed by collaborations with many colleagues, coworkers, and students. I would like to express sincere thanks to all those people, in particular, Prof. Emer. Syûzô Seki (Osaka University), who was my supervisor when I started chemical thermodynamic research, and Prof. Philipp Gütlich (Mainz University), who was my supervisor when I stayed in West Germany from 1974 to 1976 as a postdoctoral fellow to study spin-crossover phenomena by Mössbauer spectroscopy. Calorimetric studies for novel compounds and systems were possible through collaborations with Prof. Emer. Mikiharu Kamachi (Osaka University), Prof. Wolfgang Haase (Darmstadt University of Technology, Germany), Prof. Norimichi Kojima (The University of Tokyo), and Prof. Hiroshi Kitagawa (Kyushu University). Heat capacities were mainly measured by Dr. Motohiro Nakano, Dr. Yuji Miyazaki, Dr. Tadahiro Nakamoto, Mr. Norihiro Ohmae, Miss Tomoko Kawamura, Miss Hisako Hara (Osaka University), Prof. Zhi-cheng Tan (Dalian Institute of Chemical Physics, China), Prof. Qi Wang (Zhejiang University, China), and Dr. Ashis Bhattacharjee (St. Joseph's College, India).

## REFERENCES


1. M. Sorai and D. N. Hendrickson. *Pure Appl. Chem*. **63**, 1503–1510 (1991).
2. M. Sorai. In *Molecule-based Magnetic Materials: Theory, Techniques and Application*, M. M. Turnbull, T. Sugimoto, L. K. Thompson (Ed.), Chap. 7, pp. 99–114, ACS Symposium Series 644, American Chemical Society, Washington, DC (1996).
3. M. Sorai, Y. Miyazaki, T. Hashiguchi. In *Magnetic Properties of Organic Materials*, P. M. Lahti (Ed.), Chap. 23, pp. 475–490, Marcel Dekker, New York (1999).
4. M. Sorai. *Bull. Chem. Soc. Jpn*. **74**, 2223–2253 (2001).
5. M. Sorai. *J. Chem. Thermodyn*. **34**, 1207–1253 (2002).
6. M. Sorai. In *Spin Crosover in Transition Metal Compounds III*, Series: Topics in Current Chemistry, Vol. 235, P. Gütlich and H. A. Goodwin (Eds.), pp. 153–170, Springer, Berlin (2004),
7. H. Sugimoto, H. Aota, A. Harada, Y. Morishima, M. Kamachi, W. Mori, M. Kishita, N. Ohmae, M. Nakano, M. Sorai. *Chem. Lett*. 2095–2098 (1991).
8. M. Kamachi, H. Sugimoto, A. Kajiwara, A. Harada, Y. Morishima, W. Mori, N. Ohmae, M. Nakano, M. Sorai, Y. Kobayashi, K. Amaya. *Mol. Cryst. Liq. Cryst*. **232**, 53–60 (1993).
9. N. Ohmae, A. Kajiwara, Y. Miyazaki, M. Kamachi, M. Sorai. *Thermochim. Acta* **267**, 435–444 (1995).
10. T. Kobayashi, M. Takiguchi, K. Amaya, H. Sugimoto, A. Kajiwara, A. Harada, M. Kamachi. *J. Phys. Soc. Jpn*. **62**, 3239–3243 (1993).
11. H. Hara and M. Sorai. *J. Phys. Chem. Solids* **56**, 223–232 (1995).
12. H. Kitagawa, N. Onodera, T. Sonoyama, M. Yamamoto, T. Fukawa, T. Mitani, M. Seto, Y. Maeda. *J. Am. Chem. Soc*. **121**, 10068–10080 (1999).
13. H. Kitagawa, N. Onodera, J.-S. Ahn, T. Mitani, K. Toriumim M. Yamashita. *Synth. Met*. **86**, 1931–1932 (1997).
14. Y. Miyazaki, Q. Wang, A. Sato, K. Saito, M. Yamamoto, H. Kitagawa, T. Mitani, M. Sorai. *J. Phys. Chem. B* **106**, 197–202 (2002).
15. K. Falk, R. Werner, Z. Tomkowicz, M. Bałanda, W. Haase. *J. Magn. Magn. Mater*. **196–197**, 564–565 (1999).
16. M. Bałanda, K. Falk, K. Griesar, Z. Tomkowicz, W. Haase. *J. Magn. Magn. Mater*. **205**, 14–26 (1999).
17. A. Bhattacharjee, K. Falk, W. Haase, M. Sorai. *J. Phys. Chem. Solids* **66**, 147–154 (2005).
18. T. Kawamura, Y. Miyazaki, M. Sorai. *Chem. Phys. Lett*. **273**, 435–438 (1997).
19. J. J. Mayerle, J. B. Torrance, J. I. Crowley. *Acta Cryst. B* **35**, 2988–2995 (1979).
20. M. Le Cointe, M. H. Lemée-Cailleau, H. Cailleau, B. Toudic, L. Toupet, G. Heger, F. Moussa, P. Schweiss, K. H. Kraft, N. Karl. *Phys. Rev. B* **51**, 3374–3386 (1995).
21. *Spin Crossover in Transition Metal Compounds I, II, III*, Series: Topics in Current Chemistry, Vols. 233, 234, 235), P. Gütlich and H. A. Goodwin (Eds.), Springer, Berlin (2004).
22. M. Sorai and S. Seki. *J. Phys. Soc. Jpn.* **33**, 575 (1972).
23. M. Sorai and S. Seki. *J. Phys. Chem. Solids* **35**, 555–570 (1974).
24. T. Nakomoto, Z.-C. Tan, M. Sorai. *Inorg. Chem*. **40**, 3805–3809 (2001).
25. P. E. Doan and B. R. McGarvey. *Inorg. Chem.* **29**, 874–876 (1990).
26. M. Sorai, Y. Yumoto, D. M. Halepoto, L. F. Larkworthy. *J. Phys. Chem. Solids* **54**, 421–430 (1993).
27. N. Kojima, W. Aoki, M. Seto, Y. Kobayashi, Yu. Maeda. *Synth. Met.* **121**, 1796–1797 (2001).
28. N. Kojima, W. Aoki, M. Itoi, Y. Ono, M. Seto, Y. Kobayashi, Yu. Maeda. *Solid State Commun.* **120**, 165–170 (2001).
29. T. Nakamoto, Y. Miyazaki, M. Itoi, Y. Ono, N. Kojima, M. Sorai. *Angew. Chem., Intl. Ed*. **40**, 4716–4719 (2001).